Eur Biophys J (2003) 32: 113–121
DOI 10.1007/s00249-002-0272-9

ARTICLE

Anurag Varshney · M.K. Mathew

Inward and outward potassium currents through the same chimeric human Kv channel

Received: 30 August 2002 / Revised: 21 November 2002 / Accepted: 21 November 2002 / Published online: 4 February 2003

Abstract Voltage-gated ion channels are among the most intensely studied membrane proteins today and a variety of techniques has led to a basic mapping of functional roles onto specific regions of their structure. The architecture of the proteins appears to be modular and segments associated with voltage sensing and the pore lining have been identified. However, the means by which movement of the sensor is transduced into channel opening is still unclear. In this communication, we report on a chimeric potassium channel construct which can function in two distinct operating voltage ranges, spanning both inward and outward currents with a non-conducting intervening regime. The observed changes in operating range could be brought about by perturbing either the direction of sensor movement or the process of transducing movements of the sensor into channel opening and closing. The construct could thus provide a means to identify the machinery underlying these processes.

Keywords Activation · Mutagenesis · Potassium channel · Voltage sensing

Introduction

The generation of action potentials requires alternation of permeability of the membrane by several orders of magnitude over a limited range of transmembrane potentials (Hille 2001). Voltage-gated potassium channels (Kv channels) are tetrameric assemblies, each subunit of which has six transmembrane segments and a re-entrant loop. Extensive domain swap and mutagenesis work has led to a basic mapping of specific functions onto distinct regions of the sequence (Holmgren et al. 1998; Yellen 1998). The fourth transmembrane segment (S4) moves in response to changes in the transmembrane electrical potential and serves as the voltage sensor (Bezanilla 2000; Cha et al. 1999; Mannuzzu et al. 1996), while the movements of the fifth and sixth helices (S5, S6) have been implicated in channel opening and closing (Holmgren et al. 1998; Yellen 1998). All Kv channels open on depolarization and thus mediate outward flux of potassium ions. However, the detailed mechanics of the manner in which movement of the voltage sensor S4 is transduced into S5-S6 movement, and hence channel opening, is unknown.

Both N- and C- termini are cytoplasmic and a growing body of evidence suggests that they interact with each other (Schulteis et al. 1996) and with the transmembrane region to modulate Kv channel assembly, gating and permeation (Hopkins et al. 1994). The extreme N-terminus mediates inactivation in rapidly inactivating channels, like Kv1.4, by the ''ball and chain'' mechanism (Zagotta et al. 1990). A more distal N-terminal region, the T1 domain, is critical for the specificity of subunit-subunit interactions (Shen and Pfafinger 1995). Three-dimensional structures of both the N-terminal ''ball'' and the T1 domains of several channels are now available (Antz et al. 1997; Kreusch et al. 1998). Deletions in the N-terminus remove rapid inactivation (Chanda and Mathew 1999; Zagotta et al. 1990) and have also been shown to affect both the rate and voltage-dependence of activation (Aldrich et al. 1990; Pascual et al. 1997; VanDongen et al. 1990). Similarly, in the case of six transmembrane inward-rectifiers like KAT1 and HERG, the N-terminus influences gating and deletions in this region affect the voltage dependence of activation (Marten and Hoshi 1998; Viloria et al. 2000) and of deactivation (Wang et al. 2000). Interestingly, some amino terminal effects on activation gating can be suppressed by second-site mutations in S4, the voltage sensor (Terlau et al. 1997), suggesting an interaction between N-terminal

A. Varshney · M.K. Mathew (✉)
Laboratory of Membrane Biophysics,
National Centre for Biological Sciences,
TIFR, UAS-GKVK Campus, 560 065 Bangalore, India
E-mail: mathew@ncbs.res.in
Fax: +91-80-3636662/6675

cytoplasmic residues with the voltage sensing apparatus (Sanguinetti and Xu 1999).

Aberrant interactions brought about by domain swaps (Stocker et al. 1991) among mammalian channels can cause major perturbations in channel gating (Varshney et al. 2002). Both human Kv1.1 and hKv1.4 open on depolarization, the latter inactivating rapidly using the ''ball and chain'' mechanism (Antz et al. 1997; Ramaswami et al. 1990). The N-terminal cytoplasmic domain of human Kv1.1, spliced onto the transmembrane body of hKv1.4, results in a chimera (1N/4) which exhibits considerably greater cooperativity in gating than does hKv1.4 (Varshney and Mathew 2000). The ''reverse chimera'', with the ball and chain of hKv1.4 spliced onto the body of hKv1.1 (4N/1), has its operating range shifted so far to hyperpolarizing potentials that it functions as an inward rectifier (Chanda et al. 1999b). Here we report on a variant of the 4N/1 chimera, where the junction between the segment derived from hKv1.4 and that from hKv1.1 has been shifted so as to retain the entire T1 domain from hKv1.1 in the chimera. This chimeric channel, 4N/1T1, is closed at resting membrane potentials, but exhibits voltage-dependent currents both on depolarization and on hyperpolarization. Both inward and outward currents are blocked by the Kv1.1-specific toxin dendrotoxin, demonstrating that the pores concerned are derived from hKv1.1. The interactions responsible for the generation of this novel voltage dependence could throw light on the mechanisms underlying voltage-dependent gating in this class of channels.

Methods

Potassium channel cDNAs were cloned from human brain stem and were subcloned into pGEMA (Ramaswami et al. 1990). The 4N/1T1 chimera was constructed using the unique Sma I site 150 aa upstream from the base of S1 in hKv1.1 (44th bp from the 5'-end of the gene) and the Stu I site at 129 upstream of the base of S1 in hKv1.4 (548th bp). The resulting construct contains 183 amino acid residues of the N-terminus of hKv1.4 linked to 480 amino acid residues of hKv1.1. The T1 domain of hKv1.1 starts 20 residues downstream to Sma I. The Pst I (115 bp in hKv1.4)-Sal I fragment from hKv1.4 was ligated to the Sal I-Sma I backbone of hKv1.1 in order to generate the 4Nb/1T1 chimera, containing 39 N-terminal aa residues (the ball domain) (Antz et al. 1997) of hKv1.4 linked in frame to 480 aa residues of hKv1.1. All mutagenesis was confirmed by sequencing the constructs on an ABI PRISM-310 automated sequencer. Methods of *Xenopus* oocyte retrieval and their maintenance have been previously described (Ramaswami et al. 1990; Varshney et al. 2002). Capped polyadenylated RNA of all the constructs was generated using T7 RNA polymerase (mMessage mMachine transcription kit, Ambion, USA). Transcribed RNA (46 nL, 150–300 ng/μL) was injected per oocyte 48 h prior to recording. RNA injection, two-electrode voltage clamp of *Xenopus* oocytes, and data analysis were carried out as described earlier (Ramaswami et al. 1990; Varshney et al. 2002). Voltage-dependent activation and inactivation curves are the best fits to the Boltzmann functions, as explained previously (Ramaswami et al. 1990). Dendrotoxin-K (Alomone Labs, Israel) was delivered from a 2 μM stock made in 10 mM HEPES (pH 7.6) containing 0.1 mg/mL BSA. All experiments were performed at room temperature.

Results

We have previously shown that *Xenopus* oocytes, microinjected with human Kv1.1 or hKv1.2 message, exhibit non-inactivating outward currents on depolarization, while hKv1.4-expressing oocytes exhibit rapidly inactivating outward currents (Ramaswami et al. 1990). Figure 1 presents schematic representations of the transmembrane topologies of hKv1.1, hKv1.4 and the chimeric constructs 4N/1T1 and 4Nb/1T1, along with the current traces observed on subjecting oocytes expressing the parental channels to depolarizing voltage pulses. The rapid inactivation seen in hKv1.4 is due to its N-terminal ''ball and chain'', as demonstrated by loss of inactivation on deleting this structure (Antz et al. 1997; Chanda and Mathew 1999). The 4N/1T1 chimera was constructed with the chimera junction placed 150

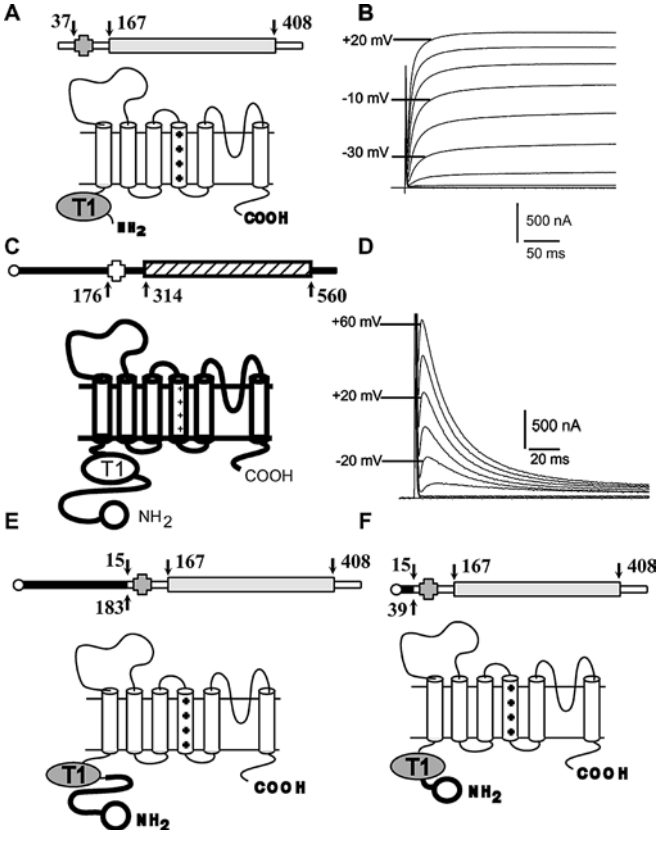

Fig. 1A–F Schematic representation of K^+ channel topologies. Transmembrane topologies and bar representations of **A** hKv1.1, **C** hKv1.4 and **E** a chimera 4N/1T1 generated by transplanting 183 residues from the N-terminus of hKv1.4 on to hKv1.1, and **F** a chimera 4Nb/1T1 generated by transplanting 39 N-terminal residues (the ball domain) from hKv1.4 on to the transmembrane body of hKv1.1. In *bar* diagrams, *arrows* and *numbers* indicate residues at the junctions of the chimeric constructs. For hKv1.1 (*down arrows*) and hKv1.4 (*up arrows*) the arrows indicate the start of T1 domain and also the transmembrane region with *residue numbers*. Intact T1 domains are depicted with a *solid cross*. **B**, **D** Currents elicited in oocytes expressing **B** hKv1.1 and **D** hKv1.4 on depolarization from −80 mV following a hyperpolarizing prepulse of 1 s to −120 mV. Potentials are indicated against the traces

residues from the base of S1 in hKv1.1, which leaves the T1 domain of hKv1.1 (residues 37–129) intact in the construct.

Outward currents through 4N/1T1

A chimera made from two outward-rectifying K^+ channels is expected to permit K^+ efflux on depolarization and 4N/1T1-expressing oocytes do, indeed, exhibit rapidly inactivating outward currents on depolarization (Fig. 2A). The rapid inactivation indicates that hKv1.1 has a functional receptor for the hKv1.4 "ball". Recovery from inactivation (i.e. unbinding of the ball) is faster in the chimera than in hKv1.4 (354 ms versus 470 ms half times at −100 mV), as would be expected if the affinity of binding is lower in the chimera (Fig. 2D). The rates of inactivation of hKv1.4 and the chimera are similar over a range of potentials (inset to Fig. 2A), as is the voltage dependence of steady-state inactivation (Fig. 2C). The voltage dependence of channel opening is expected to be controlled by machinery residing within the transmembrane region, all of which is derived from hKv1.1. Figure 2B analyses outward currents through the chimera and compares it to the voltage dependence of the parental channels. As expected, the voltage dependence of the 4N/1T1 chimera is essentially identical to that of hKv1.1, with a mid point of activation at −30 mV.

The pore of the chimera is contributed by hKv1.1 and so is expected to be potassium selective and sensitive to Kv1.1-specific blockers. Selectivity can be estimated from the reversal potential of the currents

Fig. 2A–D Outward currents through 4N/1T1. **A** Currents from oocytes expressing 4N/1T1 channels in response to depolarizing pulses from a holding potential of −80 mV. *Inset*: time constant for inactivation of 4N/1T1 (*open circles*) and hKv1.4 (*solid circles*) as a function of transmembrane potential. The data have been fitted to single exponentials with decay constants of 15.63 mV and 15.78 mV for the chimera (*open circles*) and hKv1.4 (*solid circles*), respectively. **B** Voltage-dependent activation of the 4N/1T1 chimera (*open circles*), hKv1.1 (*solid squares*) and hKv1.4 (*solid circles*), fitted to the Boltzmann functions. $V_{1/2}$ of activation for hKv1.1 (*solid squares*) and 4N/1T1 (*open circles*) are −29.2 mV and −30.5 mV, respectively. hKv1.4 conductance does not reach saturation (Varshney and Mathew 2000) and so the value of $V_{1/2}$ obtained depends on the highest depolarizing potential in the experimental protocol. **C** Voltage dependence of inactivation of 4N/1T1 chimera. The membrane potential was stepped from a holding potential of −80 mV to a series of depolarizing conditioning pulses ranging from −80 mV to +20 mV for 600 ms. The steady-state inactivated channels were then stepped to the test potential of +10 mV. The peak currents (*I*) at this test potential are plotted as a function of conditioning pulse potentials (*V*) in the *inset*. The midpoints of inactivation for 4N/1T1 chimera (*open circles*) and hKv1.4 (*solid circles*) were −45.7 mV and −51.4 mV, respectively. **D** Recovery from inactivation for 4N/1T1 chimera. The membrane potential was stepped from a holding potential of −80 mV to 0 mV for 1 s. The membrane was then hyperpolarized to −100 mV for varying periods of time before stepping back to 0 mV. Pulse trains were initiated every 10 s. *Inset*: time course of channel recovery from inactivation was fitted to single exponentials, yielding time constants of 731.25 ms and 941.64 ms for 4N/1T1 (*open circles*) and hKv1.4 (*solid circles*), respectively

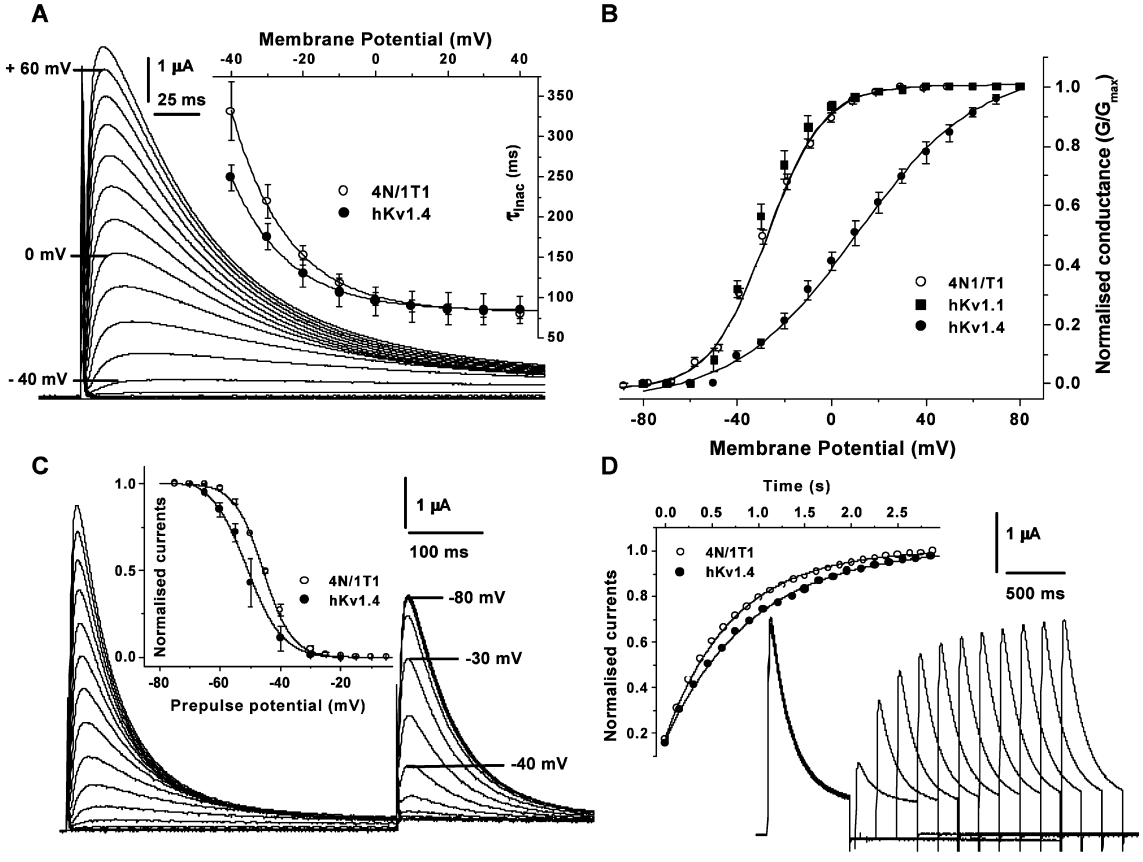

through the channels. Indeed, the reversal potential measured with 2 mM K^+ in the bathing medium is between −85 mV and −95 mV (Fig. 3A), indistinguishable from that reported for hKv1.1 (Ramaswami et al. 1990). Further, the Kv1.1-specific blocker dendrotoxin blocks currents through the chimera with an IC_{50} of 1 nM (Fig. 3B).

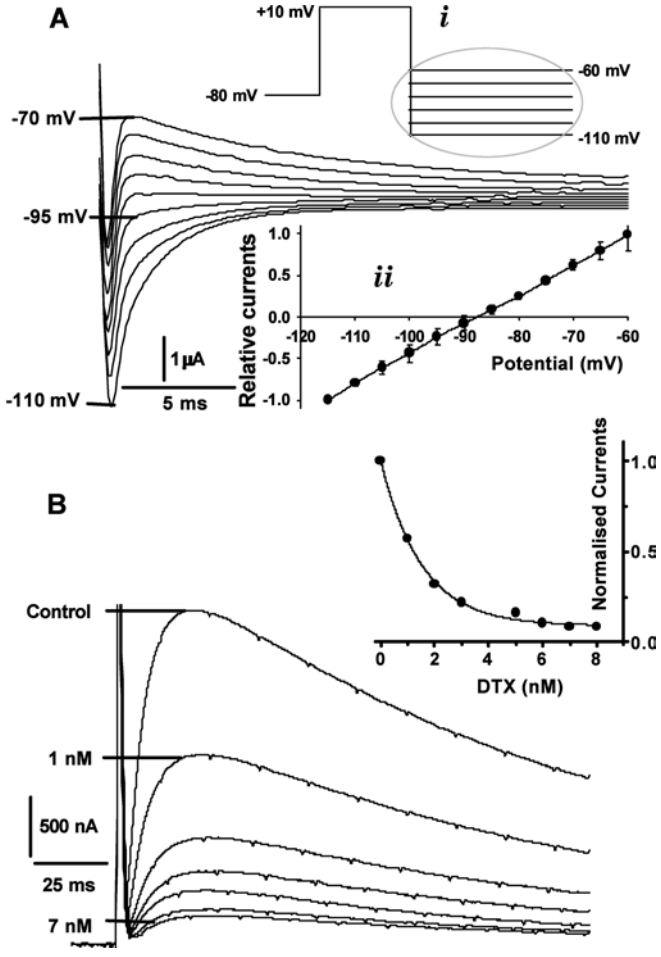

Fig. 3 Outward currents pass through the hKv1.1 pore. **A** Reversal potential for 4N/1T1 in 2 mM K^+_{out}. Channels were opened at +10 mV for 10 ms, and then stepped to different repolarizing potentials ranging from −110 mV to −60 mV for 100 ms, as shown in *inset i*. Tail current amplitude through closing channels was determined by fitting a single exponential function to the current between 5 and 100 ms after repolarization and then extrapolating back to the start of the repolarization step. The variation of this tail current amplitude with repolarizing potentials is shown in *inset ii*. **B** The concentration dependence of the dendrotoxin block of the outward current of 4N/1T1. Dendrotoxin was applied in a cumulative fashion to the oocyte-expressing 4N/1T1 chimera; the test potential was +10 mV and currents were recorded at different concentrations after the manual addition of DTX in the bath. *Inset*: the concentration dependence of the DTX block was fitted to a form of the Langmuir equation, $I/I_0 = I_0/\{1 + ([DTX]/IC_{50})\}$, where I_0 is the current in the absence of dendrotoxin, I the observed current in the presence of [DTX] at different concentrations (nM), and IC_{50} the concentration of DTX required for 50% block and was calculated to be 1 nM. *Error bars* represent standard error of the means for all data sets ($n = 3$–6)

Inward currents through the 4N/1T1 chimera

We had earlier reported on the 4N/1 chimera which functions as an inward rectifier (Chanda et al. 1999b). The 4N/1 chimera has a chimera junction within the T1 domain, in a manner expected to disrupt the tetrameric assembly of this cytoplasmic structure (Kreusch et al. 1998). Hyperpolarization of oocytes expressing 4N/1T1 results in inward currents (Fig. 4A), similar to those reported for 4N/1 (Chanda et al. 1999b). No such currents are seen on hyperpolarization of oocytes expressing hKv1.1 or hKv1.4 or the truncation construct of hKv1.1, Δ78N1, truncated close to the chimera junction (Fig. 4B).

We have used the amplitude of tail currents on stepping to −60 mV as an estimate of the number of open channels at each test potential. Tail current amplitudes are proportional to the number of channels open at the time of the potential stepping to −60 mV, at which potential the channels are closed. This data are presented in Fig. 4C and demonstrate that the current-voltage curve is non-linear, i.e. the probability of channel opening is voltage dependent.

Characterizing the pore for inward and outward currents

We have previously shown that co-expression of the "ball and chain" from hKv1.4 along with Δ78N1 of separate transcripts in the same oocyte results in inward rectifying currents, suggesting that the peptide interacts with residues on the cytoplasmic face of the channel to bring about this perturbation in operating range (Chanda et al. 1999a). We now hypothesize that the inward and outward currents we observe in 4N/1T1-expressing oocytes arise from two populations of the same chimeric channels: the inward currents from channels where the chain is bound to the cytoplasmic face of the channel, and the outward currents from channels where this interaction is absent. This hypothesis requires that the inward currents flow through the same pore as the outward currents, i.e. the hKv1.1 pore.

The Kv1.1 pore is K^+ selective and specifically blocked by dendrotoxin (DTX), a component of mamba venom (Hopkins et al. 1999; Ramaswami et al. 1990). The reversal potential for outward currents is estimated to lie between −85 mV and −95 mV (Fig. 3A), essentially the same as that reported earlier for hKv1.1 in ND96 containing 2 mM K^+_{out} (Ramaswami et al. 1990). Tail currents in Fig. 4A show that repolarizing to −65 mV results in inward currents flowing through channels that had opened on membrane hyperpolarization. The reversal potential for these channels is thus less negative than −65 mV, indicating that the channel is less K^+ selective than Kv1.1.

Dendrotoxin has been reported to block Kv1.1 channels with high affinity, with relatively little effect on

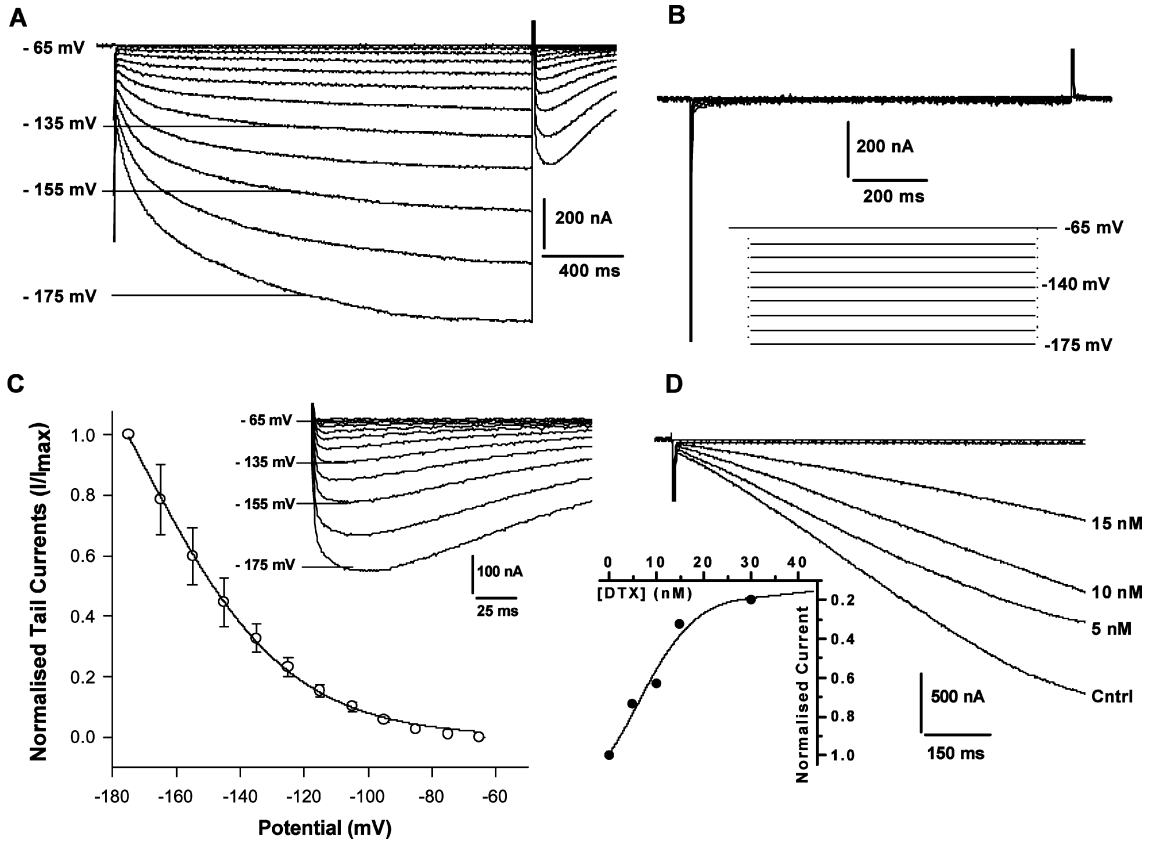

Fig. 4A–D Inward currents through 4N1/T1. Currents in oocytes expressing **A** 4N/1T1 chimera, **B** hKv1.1 or hKv1.4 or Δ78N1, in independent experiments, in response to hyperpolarizing pulses. Oocytes were held at −65 mV and stepped to hyperpolarizing potentials from −65 mV to −175 mV in 10 mV steps, as shown in the *inset* to **B**. **C** Tail currents at −65 mV from **A** fitted to a Boltzmann function, with $V_{1/2}$ of −175 mV. *Inset*: amplified currents used for the fit. **D** Effect of successive additions of DTX on inward currents. Concentrations are mentioned against the traces. Membrane potential was held at −70 mV before stepping down to −145 mV. *Inset*: dose dependence of DTX block, using the Langmuir function as described in Fig. 3B

other Kv channels (Hopkins et al. 1999). Figure 3B shows that DTX blocks outward currents through 4N/1T1 channels with an IC_{50} of 1 nM. Inward currents are also blocked by DTX, but with a lower affinity: an IC_{50} of 11 nM is estimated (Fig. 4D).

Effect of deleting the N-terminal chain

The shift in operating range of 4N/1T1 is brought about by aberrant interactions involving the ball and chain from hKv1.4. In an attempt to home in on the responsible region, we have deleted much of the chain between the "ball" structure and the T1 domain. A deletion of 144 residues, leaving only 22 residues between the two structures (as opposed to 166 in 4N/1T1), generated the 4Nb/1T1 chimera (Fig. 1F). Oocytes expressing this construct display rapidly inactivating outward currents on depolarization (Fig. 5A). The voltage dependence of activation for these currents is the same as for hKv1.1 and 4N/1T1 (inset to Fig. 5A), as expected for an unperturbed outward current. However, no inward currents are seen on hyperpolarization of oocytes expressing 4Nb/1T1 (Fig. 5C), suggesting that residues in the deleted portion are critical for the interactions leading to the shift in operating range. The "ball" portion, however, is effective in causing inactivation in the construct with a voltage dependence of inactivation similar to that of 4N/1T1 ($V_{1/2}$ of inactivation of −43 mV for 4Nb/1T1, −46 mV for 4N/1T1 and −51 mV for hKv1.4) (Fig. 5B). The rate of inactivation may be expected to vary with the length of intervening chain, as reported for the Shaker channel (Timpe and Peller 1995). However, the rates of inactivation of 4Nb/1T1, 4N/1T1 and hKv1.4 are comparable ($\tau_{inact} = 86.03$, 89.66 and 88.55 ms, respectively, at +10 mV). Recovery from inactivation, on the other hand, is expected to be independent of the chain, and reflects only the dissociation of the ball from its binding site. Indeed, recovery from inactivation at −100 mV is almost identical for the two chimeras (352 ms half-time for 4Nb/1T1 and 354 ms for 4N/1T1) and distinct from that of hKv1.4 (470 ms half-time) (Fig. 5E). The reversal potential of the construct is close to −90 mV in 2 mM extracellular K^+, indicating a potassium-selective pore (data not shown), while outward currents are blocked by DTX with an IC_{50} of 1.1 nM (as for 4N/1T1 and hKv1.1), demonstrating that the pore is derived from hKv1.1 (Fig. 5D).

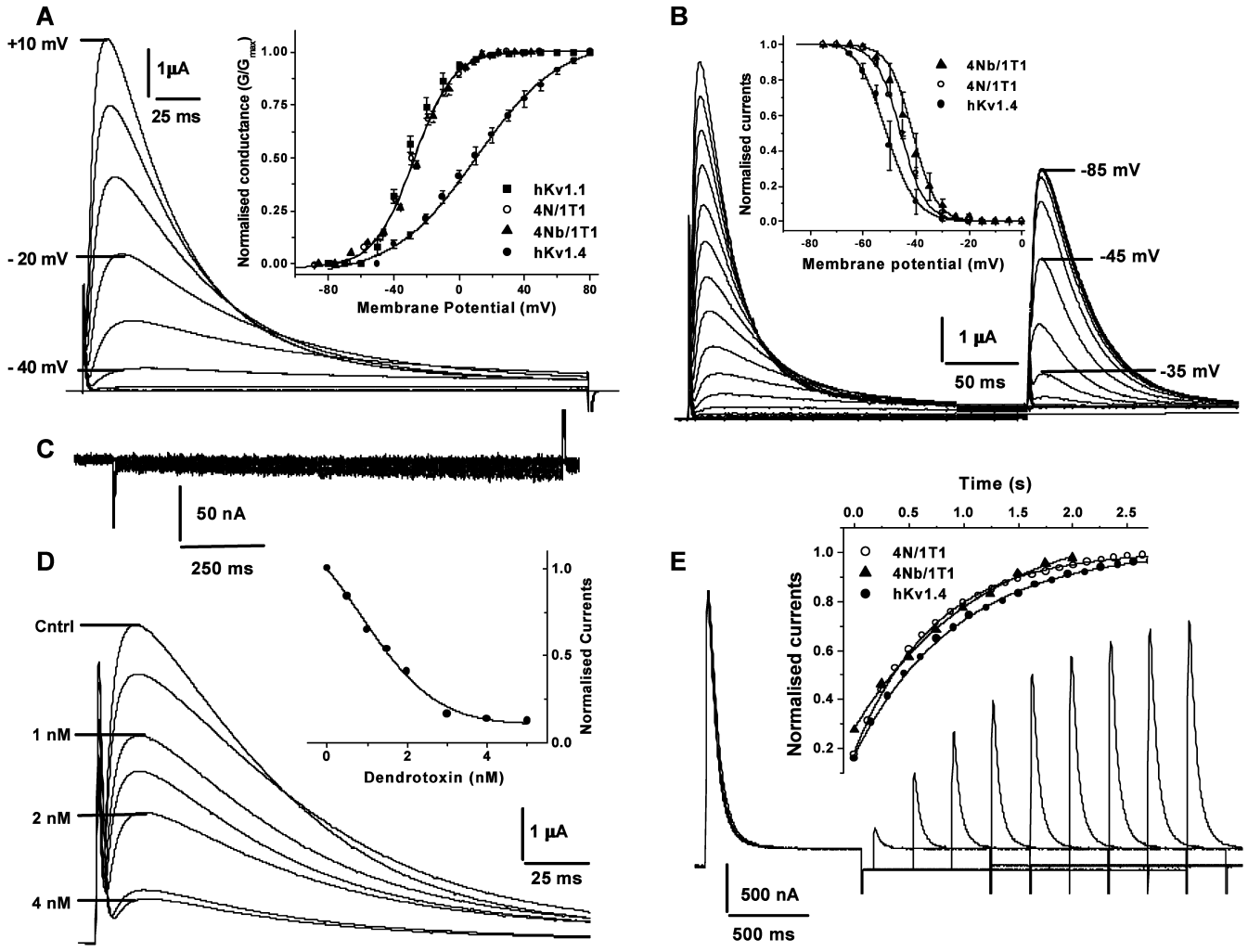

Fig. 5A–E Potassium currents from oocytes expressing 4Nb/1T1 channels. **A** Currents in response to depolarizing pulses. A hyperpolarizing prepulse to −120 mV was used prior to depolarizing to potentials indicated against the traces. *Inset*: voltage-dependent activation of the 4Nb/1T1 chimera (*solid triangles*), 4N/1T1 chimera (*open circles*), hKv1.1 (*solid squares*) and hKv1.4 (*solid circles*). The curves through data for 4Nb/1T1, 4N/1T1 and hKv1.1 are best fits to Boltzmann functions, as described in Methods. $V_{1/2}$ for hKv1.1 (*solid squares*), 4N/1T1 (*open circles*) and 4Nb/1T1 (*solid triangles*) are −29.2, −30.5 and −28.3 mV, respectively. **C** Currents observed in response to hyperpolarizing pulses. Oocytes were held at −65 mV and stepped to hyperpolarizing potentials from −65 mV to −175 mV in −10 mV steps, as shown in the inset to Fig. 4B. **D** Currents through 4Nb/1T1 pass through a Kv1.1 pore. Dendrotoxin block of outward currents, as described in Fig. 3B. *Inset*: plots of current as a function of DTX concentration, with IC_{50} at 1.1 nM. Inactivation in 4Nb/1T1 chimera. **B** Voltage dependence of inactivation, with a protocol as described in Fig. 2C. *Inset* shows the data plotted as described in Fig. 2C, with mid-points of inactivation for 4Nb/1T1 chimera (*solid triangles*), 4N/1T1 chimera (*open circles*) and hKv1.4 (*solid circles*) of −42.8, −45.7 and −51.4 mV, respectively. **E** Recovery from inactivation, as described in Fig. 2D. *Inset* shows the time dependence of channel recovery from inactivation for 4Nb/1T1 (*solid triangles*), 4N/1T1 (*open circles*) and hKv1.4 (*solid circles*)

Voltage-dependent inward and outward currents through 4N/1T1

The 4N/1T1 chimera opens on depolarization above −50 mV and on hyperpolarization below −90 mV. It should thus be possible to sample both inward and outward currents by stepping to test potentials from a holding potential in the range −90 to −50 mV. Figure 6A presents current traces from an oocyte held at −70 mV and stepped to both depolarizing and hyperpolarizing potentials. Figure 6B presents the normalized current-voltage relationship observed for these channels. The conductance is clearly non-linear in both the outward and inward directions, with an intervening non-conducting zone. The probabilities of channel opening in both directions are combined in Fig. 6C. The two sets of data have been fit independently to Boltzmann functions for consistency, although we could not sample inward currents at sufficiently hyperpolarizing potentials for a complete curve. The mid-points of the fits lie at −30 mV and −175 mV for the outward and inward currents, respectively.

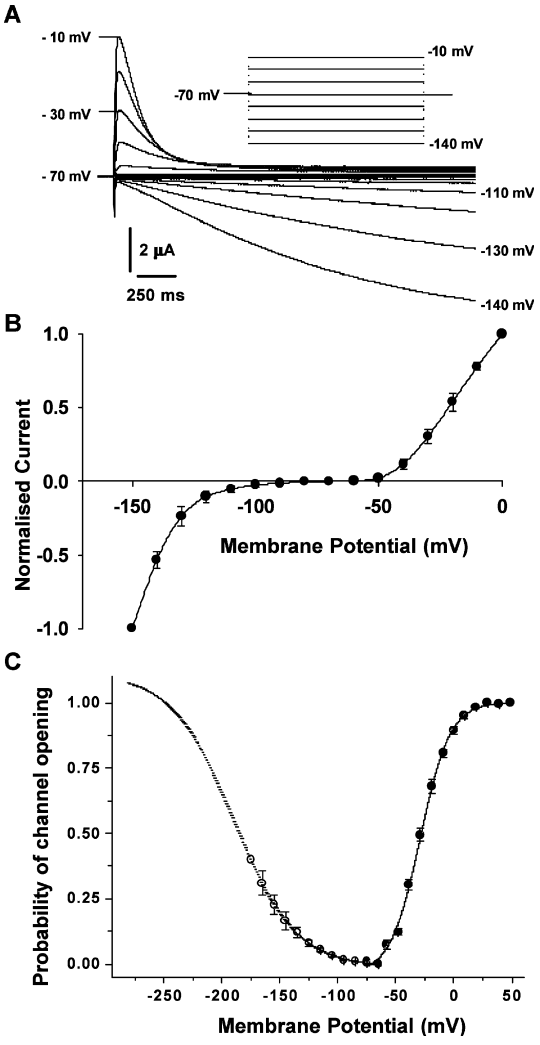

Fig. 6A–C Inward and outward currents through the same channels. **A** Currents through an oocyte expressing 4N/1T1 held at −70 mV and stepped to a range of potentials from +30 mV to −140 mV, as shown in the *inset*. **B** Current-voltage relationship for the data from **A** and averaged over three oocytes. **C** Probability of channel opening as a function of membrane potential for both inward (*dotted line*) and outward (*solid line*) currents using the protocols in Figs. 2 and 4. Both inward and outward currents are fitted to Boltzmann functions with mid points of −30 mV (outward currents) and −175 mV (inward currents)

Discussion

The initial analysis of the sequence of the sodium channel identified the S4 transmembrane helices, with positively charged residues at every third location, as putative voltage sensors. This hypothesis was later confirmed (Stuhmer et al. 1989) and has been extensively investigated in sodium, potassium and calcium channels (Hille 2001). Movements of S4 helices in response to depolarizing pulses have been detected in terms of differential accessibility of residues in the "open" versus the "closed" state (Mannuzzu et al. 1996), of changes in the environment of fluorophores attached to these sites (Cha et al. 1999), and of changes in distance between these fluorophores (Glauner et al. 1999), or by histidine scanning mutagenesis (Starace and Bezanilla 2001). Analysis of gating current measurements in Shaker channels has resulted in models of gating which involve independent movement of sensors in each subunit, followed by a late cooperative transition leading to channel opening (Ledwell and Aldrich 1999; Schoppa and Sigworth 1998). There is, as yet, no clear understanding as to how movements of the S4 helix are transduced into movements of the S5 and S6 helices and thus channel opening (Papazian 1999).

Shifts in voltage sensitivity of K^+ channels have been generated mainly by mutations in S4. The largest such shifts have been brought about not by mutations in the charged residues but rather by mutations in apolar residues as in the V2 (L382V) (Schoppa and Sigworth 1998) and ILT (V369I, I372L and S376T) (Ledwell and Aldrich 1999) mutants of Shaker. The quantum of gating charge moving across the electric field is unaffected in these mutants, as is the voltage range over which much of the charge moves. However, the range over which the final cooperative transitions occur is shifted to the range where ionic currents are seen (Ledwell and Aldrich 1999; Schoppa and Sigworth 1998). It would be reasonable to assume that these mutations affect the process by which voltage sensing (the bulk of the charge movement seen in gating current measurements) is transduced into channel opening (Loboda and Armstrong 2001), probably associated with the much smaller charge movement seen later.

A large shift in operating range of a Shaker-type channel occurs in the 4N/1 and 4N/1T1 chimeras. In neither case is the shift due to the absence of the native tail, as a control construct truncated close to the splice junctions functions just like full-length hKv1.1 (Fig. 4B and Chanda et al. 1999b). The residues on the foreign tail that are critical for this aberrant interaction lie between the "ball" structure and the T1 domain, as demonstrated by the inability of a chimeric construct lacking these residues to generate inward currents on hyperpolarization (Fig. 5).

Six-transmembrane inward rectifiers like HERG, HCN1 and KAT1 could, in principle, function in one of two ways by having their voltage sensors move inwards on hyperpolarization, or by retaining the direction of voltage-sensor movement but shifting the transition far into the hyperpolarizing range. In the latter case, channels would need to be kept in an inactive state at resting membrane potentials and recover from inactivation on hyperpolarization, as suggested by Yellen and coworkers (Smith et al. 1996) and by Miller and Aldrich (1996). The latter authors have shown that Shaker channels can be converted to inward rectifiers by introducing mutations in their S4 helices, with voltage dependence of conductance consistent with the inactivation gating mechanism (Miller and Aldrich 1996). However, in a recent study on KAT1, Latorre et al. (2001) have reported inward gating currents on taking

KAT1 through its gating transition, consistent with its S4 moving in the sense opposite to that of Shaker. Considering that the sequence of S4 in KAT1 is similar to that in Shaker, the observation of inward but not outward gating currents in KAT1, and the reverse in Shaker, would imply mechanisms for limiting sensor movements in the undesired direction. Shifting of the operating range of 4N/1T1 would thus require perturbation of either the apparatus that limits S4 movements, or the machinery that transduces these movements into channel opening. A perturbant of either process should provide a handle for the identification of the components involved.

One possible means by which two populations of channels could have been generated would be to have some of them inserted "upside-down", i.e. with their transmembrane topology inverted. However, dendrotoxin (DTX), a snake toxin with a high affinity site on the extracellular turret of hKv1.1, is effective in blocking both inward and outward currents (Figs. 3B and 4D). DTX is added to the bath and, being polar, is unlikely to be membrane permeant. Hence this result would imply that both populations of channels have their "turrets" on the extracellular surface of the oocytes. DTX binding further establishes that the pore through which current passes in the inward rectifying population is derived from hKv1.1. The toxin blocks inward currents with 50% efficiency at 11 nM, while it blocks hKv1.1 and the outward currents at about 1 nM. Although the affinity for the inward rectifying population is significantly lower than for hKv1.1, it is still over three orders of magnitude higher than that for any other member of the Kv1.x family.

Recent reports on reversible interconversion of a leak potassium channel, KCNK2, into a voltage-dependent channel on phosphorylation (Bockenhauer et al. 2001), and point mutations in the S4-S5 linker which transform an inward rectifier, pacemaker (HCN) channel, into a voltage-independent constitutively open channel (Chen et al. 2001), describe channels which can mediate inward and outward flux of potassium under suitable conditions. Here we report on the 4N1/T1 chimera which exhibits voltage dependence of conductance in both regimes without covalent modification required for the interconversion. This physiology, while unusual, is not unique as Sanguinetti and Xu (1999) have reported on a mutant HERG channel that also exhibits voltage-dependent conductances on depolarization as well as on hyperpolarization.

The outward currents seen in 4N/1T1 and 4Nb/1T1 inactivate rapidly, demonstrating a binding site in hKv1.1 for the Kv1.4 "ball". Recovery from inactivation in the two constructs is similar, as expected for a dissociation reaction which should be independent of chain length. More intriguing is the relative insensitivity of the rate of inactivation to chain length. Standard structural models of the voltage-gated K^+ channels have the T1 domain suspended below the transmembrane region (Choe et al. 1999), in a "hanging gondola" architecture (Kobertz et al. 2000). The ball is suspended in the cytosol below the tetramerized T1 platform. Inactivation requires the ball to "snake" in between the T1 and the membrane to block the conducting pore (Zhou et al. 2001). At first sight, such a mechanism may be expected to be very sensitive to the length of chain between T1 and the ball. Deletion experiments, however, indicate that the length of this chain is not a major determinant of the rate of inactivation of rat Kv1.4 channels (Tseng-Crank et al. 1993). In the case of 4Nb/1T1, a chain of just 22 residues suffices to effect inactivation at rates comparable to a chain of 166 residues in 4N/1T1 or 138 residues in hKv1.4.

Inward currents are seen in the 4N/1 chimera which has hKv1.4 sequences extending into the T1 domain in a manner that is expected to disrupt the tetrameric assembly of this domain (Chanda et al. 1999b; Kreusch et al. 1998). The 4/1T1 chimera has been constructed so as to incorporate an intact T1 domain from hKv1.1 spliced onto the cytoplasmic tail from hKv1.4. While both generate inward currents on hyperpolarization, significant outward currents are seen mainly in the latter case. It would thus appear that the residues responsible for the shift in operating range reside between the N-terminus and the T1 domain of hKv1.4, while additional residues from the T1 domain of hKv1.4 enhance its binding to hKv1.1. Further, the inability of the deletion construct 4Nb/1T1 to open on hyperpolarization suggests that residues in the ball structure are insufficient to cause this perturbation, i.e. the relevant residues are in the chain of hKv1.4. Thus 4Nb/1T1 opens only on depolarization and 4N/1 functions almost exclusively as an inward rectifier, with the chain bound under our experimental conditions. In the 4N/1T1 chimera that we report on here, the bound and free forms co-exist. This generates two populations of channels, one that functions as a garden-variety outward rectifier and another that functions as an inward rectifier. This switching of the operating range of the channel on chain binding could provide a handle to probe the machinery involved in either limiting the movement of the voltage-sensing apparatus or in transducing such movements into channel opening and closing. In addition, the ability to tune the operating range of the channel to either inward or outward rectification interspersed with a substantial non-conducting regime may permit its use in designing switching elements in bio-electrical circuits.

Acknowledgements The authors thank Drs. J.B. Udgaonkar, B. Chanda and U.S. Bhalla for comments on the manuscript. The authors also thank S. Kavitha for her help during experiments. A.V. acknowledges support from the Kanwal Rekhi Scholarship of the TIFR Endowment Fund. This work was supported by internal funds from NCBS.

References

Aldrich RW, Hoshi T, Zagotta WN (1990) Differences in gating among amino-terminal variants of Shaker potassium channels. Cold Spring Harb Symp Quant Biol 55:19–27

Antz C, Geyer M, Fakler B, Schott MK, Guy HR, Frank R, Ruppersberg JP, Kalbitzer HR (1997) NMR structure of inactivation gates from mammalian voltage-dependent potassium channels. Nature 385:272–275

Bezanilla F (2000) The voltage sensor in voltage-dependent ion channels. Physiol Rev 80:555–592

Bockenhauer D, Zilberberg N, Goldstein SA (2001) KCNK2: reversible conversion of a hippocampal potassium leak into a voltage-dependent channel. Nat Neurosci 4:486–491

Cha A, Snyder GE, Selvin PR, Bezanilla F (1999) Atomic scale movement of the voltage-sensing region in a potassium channel measured via spectroscopy. Nature 402:809–813

Chanda B, Mathew MK (1999) Functional reconstitution of bacterially expressed human potassium channels in proteoliposomes: membrane potential measurements with JC-1 to assay ion channel activity. Biochim Biophys Acta 1416:92–100

Chanda B, Tiwari JK, Varshney A, Mathew MK (1999a) Exploring the architecture of potassium channels using chimeras to reveal signal transduction. Biosci Rep 9:301–306

Chanda B, Tiwari JK, Varshney A, Mathew MK (1999b) Transplanting the N-terminus from Kv1.4 to Kv1.1 generates an inwardly rectifying K^+ channel. Neuroreport 10:237–241

Chen J, Mitcheson JS, Tristani-Firouzi M, Lin M, Sanguinetti MC (2001) The S4-S5 linker couples voltage sensing and activation of pacemaker channels. Proc Natl Acad Sci USA 98:11277–11282

Choe S, Kreusch A, Pfaffinger PJ (1999) Towards the three-dimensional structure of voltage-gated potassium channels. Trends Biochem Sci 24:345–349

Glauner KS, Mannuzzu LM, Gandhi CS, Isacoff EY (1999) Spectroscopic mapping of voltage sensor movement in the Shaker potassium channel. Nature 402:813–817

Hille B (2001) Ionic channels of excitable membranes, 3rd edn. Sinauer, Sunderland, Mass., USA

Holmgren M, Shin KS, Yellen G (1998) The activation gate of a voltage-gated K^+ channel can be trapped in the open state by an intersubunit metal bridge. Neuron 21:617–621

Hopkins WF, Demas V, Tempel BL (1994) Both N- and C-terminal regions contribute to the assembly and functional expression of homo- and heteromultimeric voltage-gated K^+ channels. J Neurosci 14:1385–1393

Hopkins WF, Allen M, Tempel BL (1999) Interactions of snake dendrotoxins with potassium channels. Methods Enzymol 294:649–661

Kobertz WR, Williams C, Miller C (2000) Hanging gondola structure of the T1 domain in a voltage-gated K^+ channel. Biochemistry 39:10347–10352

Kreusch K, Pfaffinger PJ, Stevens CF, Choe S (1998) Crystal structure of the tetramerization domain of Shaker potassium channel. Nature 392:945–948

Latorre R, Basso C, Gonzalez C, Alvarez O, Cosmelli D (2001) KAT1, a K^+ channel from *Arabidopsis thaliana*, possesses an intrinsic voltage sensor. Biophys J 80:436a

Ledwell JL, Aldrich RW (1999) Mutations in the S4 region isolate the final voltage-dependent cooperative step in potassium channel activation. J Gen Physiol 113:389–414

Loboda A, Armstrong CM (2001) Resolving the gating charge movement associated with late transitions in K^+ channel activation. Biophys J 81:905–916

Mannuzzu LM, Moronne MM, Isacoff EY (1996) Direct physical measure of conformational rearrangement underlying potassium channel gating. Science 271:213–216

Marten I, Hoshi T (1998) The N-terminus of the K channel KAT1 controls its voltage-dependent gating by altering the membrane electric field. Biophys J 74:2953–2962

Miller AG, Aldrich RW (1996) Conversion of a delayed rectifier K^+ channel to a voltage-gated inward rectifier K^+ channel by three amino acid substitutions. Neuron 16:853–858

Papazian DM (1999) Potassium channels: some assembly required. Neuron 23:7–10

Pascual JM, Shieh CC, Kirsch GE, Brown AM (1997) Contribution of the NH_2 terminus of Kv2.1 to channel activation. Am J Physiol 273:C1849–C1858

Ramaswami M, Gautam M, Kamb A, Rudy B, Tanouye MA, Mathew MK (1990) Human potassium channel genes: molecular cloning and functional expression. Mol Cell Neurosci 1:214–223

Sanguinetti MC, Xu QP (1999) Mutations of the S4-S5 linker alter activation properties of HERG potassium channels expressed in *Xenopus* oocytes. J Physiol (Lond) 514:667–675

Schoppa NE, Sigworth FJ (1998) Activation of Shaker potassium channels. III. An activation gating model for wild-type and V2 mutant channels. J Gen Physiol 111:313–342

Schulteis CT, Nagaya N, Papazian DM (1996) Intersubunit interaction between amino- and carboxyl-terminal cysteine residues in tetrameric Shaker K^+ channels. Biochemistry 35:12133–12140

Shen NV, Pfafinger PJ (1995) Molecular recognition and assembly sequences involved in the subfamily-specific assembly of voltage-gated K^+ channel subunit proteins. Neuron 14:625–633

Smith PL, Baukrowitz T, Yellen G (1996) The inward rectification mechanism of the HERG cardiac potassium channel. Nature 379:833–836

Starace DM, Bezanilla F (2001) Histidine scanning mutagenesis of basic residues of the S4 segment of the Shaker K^+ channel. J Gen Physiol 117:469–490

Stocker M, Pongs O, Hoth M, Heinemann SH, Stuhmer W, Schroter KH, Ruppersberg JP (1991) Swapping of functional domains in voltage-gated K^+ channels. Proc R Soc Lond Ser B 245:101–107

Stuhmer W, Conti F, Suzuki H, Wang XD, Noda M, Yahagi N, Kubo H, Numa S (1989) Structural parts involved in activation and inactivation of the sodium channel. Nature 339:597–603

Terlau H, Heinemann SH, Stuhmer W, Pongs O, Ludwig J (1997) Amino terminal-dependent gating of the potassium channel rat eag is compensated by a mutation in the S4 segment. J Physiol (Lond) 502:537–543

Timpe LC, Peller L (1995) A random flight chain model for the tether of the Shaker K^+ channel inactivation domain. Biophys J 69:2415–2418

Tseng-Crank J, Yao JA, Berman MF, Tseng GN (1993) Functional role of the NH_2-terminal cytoplasmic domain of a mammalian A-type K^+ channel. J Gen Physiol 102:1057–1083

VanDongen AM, Frech GC, Drewe JA, Joho RH, Brown AM (1990) Alteration and restoration of K^+ channel function by deletions at the N- and C-termini. Neuron 5:433–443

Varshney A, Mathew MK (2000) Cytoplasmic residues influence the voltage-dependence of the gating of human K^+ channels. Neuroreport 11:2913–2917

Varshney A, Kavitha S, Mathew MK (2002) Modulation of voltage sensitivity by N-terminal cytoplasmic residues in human Kv1.2 channels. Eur Biophys J 31:365–372

Viloria CG, Barros F, Giraldez T, Gomez-Varela D, de la Pena P (2000) Differential effects of amino-terminal distal and proximal domains in the regulation of human erg K^+ channel gating. Biophys J 79:231–246

Wang J, Myers CD, Robertson GA (2000) Dynamic control of deactivation gating by a soluble amino-terminal domain in HERG K^+ channels. J Gen Physiol 115:749–758

Yellen G (1998) The moving parts of voltage-gated ion channels. Q Rev Biophys 31:239–295

Zagotta WN, Hoshi T, Aldrich RW (1990) Restoration of inactivation in mutants of Shaker potassium channels by a peptide derived from ShB. Science 250:568–571

Zhou M, Morais-Cabral JH, Mann S, MacKinnon R (2001) Potassium channel receptor site for the inactivation gate and quaternary amine inhibitors. Nature 411:657–661